

Different rescattering trajectories related to different total electron momenta in nonsequential double ionization

Phay J. Ho and J. H. Eberly

Department of Physics and Astronomy, University of Rochester, Rochester NY 14627, USA

phayho@pas.rochester.edu

Abstract: We extend earlier work on two-electron photo-ionization to analyze electron momentum. We provide theoretical evidence distinguishing two categories of e-e trajectory associated with the correlation that develops when an “outer” electron returns to the nucleus in the presence of a high-intensity optical-wavelength laser field. We use the method of back-analysis to connect these two categories of trajectory with NSDI events having either nearly zero (Z) or substantially non-zero (NZ) total electron momentum.

© 2003 Optical Society of America

OCIS codes: (270.4180) Multiphoton processes; (270.6620) Strong-field processes; (260.3230) Ionization

References and links

1. D. N. Fittinghoff *et al.*, “Observation of nonsequential double ionization of Helium with optical tunneling,” *Phys. Rev. Lett.* **69**, 2642 (1992).
2. B. Walker *et al.*, “Precision measurement of strong field double ionization,” *Phys. Rev. Lett.* **73**, 1227 (1994).
3. B. Sheehy *et al.*, “Single- and multiple-electron dynamics in the strong-field tunneling limit,” *Phys. Rev. A* **58**, 3942 (1998).
4. Th. Weber *et al.*, “Correlated electron emission in multiphoton double ionization,” *Nature (London)* **405**, 658 (2000).
5. M. V. Ammosov, N. B. Delone, and V. P. Krainov, “Tunnel ionization of complex atoms and of atomic ions in an alternating electromagnetic field,” *Sov. Phys. JETP* **64**, 1191 (1986).
6. K. J. Schafer *et al.*, “Above threshold ionization beyond the high harmonic cutoff,” *Phys. Rev. Lett.* **70**, 1599 (1993).
7. Baorui Yang *et al.*, “Intensity-dependent scattering rings in high order above-threshold ionization,” *Phys. Rev. Lett.* **71**, 3770 (1993).
8. K. T. Taylor, J.S. Parker, D. Dundas, K.J. Meharg, L.R. Moore and J.F. McCann, “Laser-driven helium, H_2^+ and H_2 ,” *J. Mod. Optics* **50**, 401 (2003).
9. J. Javanainen, J.H. Eberly and Q. Su, “Numerical simulations of multiphoton ionization and above-threshold electron spectra,” *Phys. Rev. A* **38**, 3430-3446 (1988).
10. R. Grobe and J.H. Eberly, “Photoelectron spectra for a two-electron system in a strong laser field,” *Phys. Rev. Lett.* **68**, 2905-2908 (1992).
11. W. -C. Liu, J. H. Eberly, S. L. Haan and R. Grobe, “Correlation effects in two-electron model atoms in intense laser fields,” *Phys. Rev. Lett.* **83**, 520 (1999).
12. See K. J. Schafer, Baorui Yang, L. F. DiMauro, and K. C. Kulander, “Above threshold ionization beyond the high harmonic cutoff,” *Phys. Rev. Lett.* **70**, 1599 (1993).
13. P. B. Corkum, “Plasma perspective on strong-field multiphoton ionization,” *Phys. Rev. Lett.* **71**, 1994 (1993).
14. H. W. van der Hart and K. Burnett, “Recollision model for double ionization of atoms in strong laser fields,” *Phys. Rev. A* **62**, 013407 (2000).
15. U. Eichmann *et al.*, “Collective multielectron tunneling ionization in strong fields,” *Phys. Rev. Lett.* **84**, 3550 (2000).
16. B. Feuerstein *et al.*, “Separation of recollision mechanisms in nonsequential strong field double ionization of Ar: the role of excitation tunneling,” *Phys. Rev. Lett.* **87**, 043003 (2001).

17. A. Becker and F.H.M. Faisal, "Interpretation of momentum distribution of recoil ions from laser induced nonsequential double ionization," Phys. Rev. Lett. **84**, 3546 (2000).
18. R. Kopold *et al.*, "Routes to nonsequential double ionization," Phys. Rev. Lett. **85** 3781 (2000).
19. S. P. Goreslavski and S. V. Popruzhenko, "Nonsequential double ionization: a quasiclassical analysis of the Keldysh-type transition amplitude," Opt. Express **8**, 395 (2001), <http://www.opticsexpress.org/abstract.cfm?URI=OPEX-8-7-395>.
20. Li-Bin Fu, Jie Liu, and Shi-Gang Chen, "Correlated electron emission in laser-induced nonsequential double ionization of Helium," Phys. Rev. A **65**, RC021406 (2002).
21. A. Becker and F. H. M. Faisal, "Interplay of electron correlation and intense field dynamics in the double ionization of helium," Phys. Rev. A **59**, R1742 (1999).
22. Th. Weber *et al.*, "Recoil-ion momentum distributions for single and double ionization of Helium in strong laser fields," Phys. Rev. Lett. **84**, 443(2000).
23. Th. Weber *et al.*, "Sequential and nonsequential contributions to double ionization in strong laser fields," J. Phys. B **33**, L127(2000).
24. R. Panfili, S. L. Haan, and J. H. Eberly, "Slow-down collisions and nonsequential double ionization in classical simulations," Phys. Rev. Lett. **89**, 113001 (2002).
25. S.L. Haan, P.S. Wheeler, R. Panfili and J.H. Eberly, "Origin of correlated electron emission in double ionization of atoms," Phys. Rev. A **66**, 061402 (2002).
26. R. Panfili and, J. H. Eberly, "Comparing classical and quantum dynamics of strong-field double ionization," Opt. Express **8**, 431 (1998), <http://www.opticsexpress.org/abstract.cfm?URI=OPEX-8-7-431>.
27. H.W. van der Hart, "Sequential versus non-sequential double ionization in strong laser fields," J. Phys. B **33**, L699 (2000).
28. P.J. Ho and J.H. Eberly, in preparation.

Evidence is abundant [1–4] that two electrons participating in atomic double photo-ionization tend to become highly correlated, in a way that has been termed "non-sequential," at laser intensities above 10^{14} watts/cm². This correlation arises from electron-electron repulsion, which is the factor missing from a theory of double ionization based on a sequential application (to an atom and then to its ion) of the well-known and well-verified ADK theory of single-electron tunneling ionization [5].

As further background, one knows that when the optical intensity of a laser probe approaches 10^{14} W/cm², the response of an atomic system can no longer be treated perturbatively. In this regime, an accurate and conceptually straightforward way to handle both the coulombic and applied optical fields theoretically is to solve the time-dependent Schrödinger equation (TDSE) numerically. This has led to attractive agreement between theory and experiment in a number of one-electron phenomena [6, 7]. However, in the case of two-electron response this approach has proven to be much more challenging and TDSE results employing all relevant spatial dimensions are not available at current experimental wavelengths. This is because the memory required to store the information required for a time-dependent two-electron wavefunction for 780 nm laser light is beyond the limit of current technology [8].

For the most common experimental wavelength, two-electron TDSE results are available only with the specific "aligned-electron" Hamiltonian model [9, 10]. This takes the e-e repulsion fully into account while assuming that the laser force on the two electrons is strong enough that the most important elements of their motion are linear, along the laser polarization axis. This one-dimensional approximation appears to be justified for NSDI effects at least on a semi-quantitative basis because the aligned-electron quantum theory has already been shown [11] to be compatible with the characteristic "knee" of NSDI ion-count data.

In place of dealing with the TDSE, various approximations are being used that are based on models that can be labelled rescattering or recollision [12, 13], shakeoff [1], modified recollision [14], collective tunneling [15] and excitation tunneling [16]. S-matrix [17–19] and semi-classical calculations [20] have been applied with these models in mind. In particular, the S-matrix calculation that uses a rescattering Feynmann diagram is currently most popular because of its ability to reproduce the ionization curve as a function of intensity [21] as well as the dou-

ble peak in the recoil momentum distribution that has been reported from recent COLTRIMS experiments on doubly ionized He atoms [22]. However, the recoil momentum distribution of Ar is different, revealing a broad single peak near zero momentum [23], for which the concept of excitation tunneling was introduced as an explanation [16]. The profusion of models being advanced, particularly to explain different aspects of the momentum distribution arising from high intensity double ionization, indicates that the theoretical picture is not yet settled.

A different line of attack is suggested by results from the aligned-electron model that show unexpected close consistency between two-electron wave function calculations and two-electron classical calculations [24–26]. A very big advantage of a classical approach is its ease of calculation, allowing a wide range of intensities, frequencies and time scales to be studied. In this paper we report results from classical calculations in the NSDI domain that suggest a new view of NSDI, a view that divides the trajectories of the so-called “recollision” process [12, 13] into two distinct categories, and then relates these to properties observed in the COLTRIMS experiments.

We note that a significant technical advantage to a classical analysis is that each 2e trajectory can be integrated backward from its outgoing state to any earlier time. Then by stepwise tracking of such a trajectory forward from the earlier time, one can obtain a clear view of all stages of the evolution, in particular the evolution of an NSDI sequence. This can obviously be done in momentum as well as coordinate space and in any number of spatial dimensions. This advantage has not been widely exploited to date. Furthermore, an advantage of classical analysis so far overlooked is that it supplies evidence otherwise missing. That is, classically one obtains an actual trajectory to look at, against which the proposed interpretations of quantum results can be directly compared, since those interpretations are universally made in the language of classical trajectories – see theoretical papers mentioned already, as well as [27].

Here we report the results of tracking selected NSDI events in both two-electron coordinate space and total electron momentum space. We show that distinct NSDI categories evident in the momentum-space data have partner categories in coordinate space related to the NSDI “jets” previously studied [24, 25]. Furthermore, we clarify the distinction between the categories by showing animations of the fully time-dependent evolution of representative trajectories.

If x and p denote position and momentum, and the subscripts 1 and 2 identify the two electrons, the aligned-electron Hamiltonian of the system is given by

$$H = \frac{p_1^2}{2} + \frac{p_2^2}{2} - ZV(x_1) - ZV(x_2) + V(x_1 - x_2) + (x_1 + x_2)E(t), \quad (1)$$

where $Z = 2$ is the nuclear charge, $V(x) = 1/\sqrt{x^2 + 1}$ is the soft-coulomb so-called “Rochester potential” [9, 10] and $E(t)$ is the electric field of the laser. Our 8-cycle laser field has a trapezoidal envelope with 2 cycles of ramp-up and ramp-down, and 4 cycles of plateau, so that 8 distinct complete (roughly periodic) cycles of ionization can be monitored. We have chosen a laser frequency corresponding to the Ti:sapphire wavelength $\lambda = 780\text{nm}$ employed in most experiments. The electric field is written as $E(t) = \mathcal{E}_0 f(t) \sin \omega t$, where \mathcal{E}_0 is the maximum field strength, $f(t)$ is the trapezoidal envelope and $\omega = 0.0584$ a.u. This gives 13-photon single ionization and 39-photon double ionization of the model. Newtonian equations of motion, given previously [24] for this Hamiltonian, are adequate because the intensities employed in the experiments are well below the relativistic regime.

We use a microcanonical ensemble with 100,000 classical trajectories with energy equal to the ground state of the two-electron atom ($E_g = -2.24$ a.u.) to mimic the probability distribution of the quantum ground state in a conventional manner [24, 26]. Once the ensemble is set up, we turn on the laser and let the particles interact with it. At the end of the laser pulse, we determine which particles have doubly ionized. A two-electron atom is considered doubly ionized if both

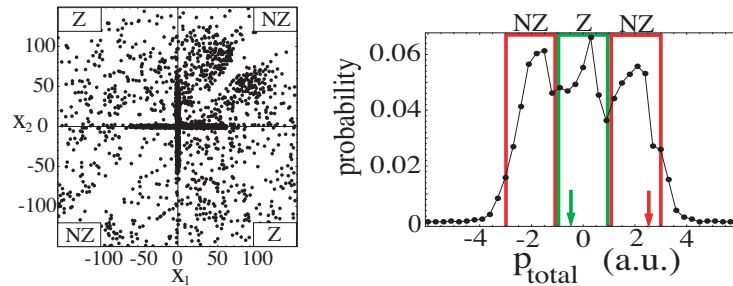


Fig. 1. On the left, two-electron NSDI trajectory points are shown in coordinate space at the end of the third cycle of the pulse. The clusters beyond 5 a.u. in the first quadrant make up the jets in NSDI, and we label each quadrant with either Z or NZ according to whether the total momentum is approximately zero or non-zero. On the right, the panel shows the final total momentum distribution of all trajectories. The green and red boxes separate the Z and NZ regions respectively. In particular, the arrows in the Z and NZ regions pinpoint the total momenta of two different trajectories that will be examined.

the electrons are free. Since the two electrons are interacting, it is not obvious how to define the energy of an individual particle. We pick out the particles that are doubly ionized using the criterion that the kinetic energy of each electron must overcome its own nuclear binding potential: $p^2/2 - ZV(x) > 0$. We have checked that letting the atoms evolve after the end of the laser pulse leads to very little change in the momentum distribution of the doubly ionized electrons. This justifies well enough our criterion.

We recall the earlier demonstration [11] that the aligned-electron theory produces the well-known “knee” structure in the ion count signal, a signal that is at least six orders of magnitude stronger than the prediction of uncorrelated ionization theory. Thus, given only 100,000 electron pairs to examine, we can expect that all ionization events will be correlated NSDI events. For this model and at this intensity, about 4% of the electrons are ionized in the short pulse.

Results from a typical classical simulation of NSDI are indicated in Fig. 1 for the laser intensity $I = 6.5 \times 10^{14}$ watts/cm². In the top row the left panel shows the NSDI 2e points at the end of the third laser cycle. A half cycle later the appearance of the 1st and 3rd quadrants would be approximately exchanged. In the right-hand panel we show the distribution of total momenta for trajectory points in the three separate regions that have the highest momentum-trajectory density. These are labelled Z or NZ according to whether their longitudinal total momentum $p_1 + p_2$ is approximately zero or non-zero.

Recently, we have developed a new method of analysis to examine various regions in total momentum distribution and relate those with features in position space. The full results will be described in another publication [28]. Our analysis shows that events producing trajectories in the jet regions of coordinate space (quadrants 1 or 3) are generally events that are found in the NZ region of total momentum. The converse is also generally true. Events producing a Z trajectory in total momentum space will generally be found in the non-jet regions (quadrants 2 or 4) of coordinate space. What is interesting is that we have found that we can relate the trajectories in these two categories to two distinct categories of two-electron evolution during the ionization process. Said differently, given the total momentum value, we must describe the “rescattering” process taking place differently for Z and NZ events. This sheds a light on rescattering that differs from the conventional one.

Conventionally a universal scenario for NSDI is adopted in which one electron is initially liberated by tunneling, to be returned to the nuclear region with energy acquired from the laser force. This energy is used to eject the second electron in a correlated way, leading to an NSDI

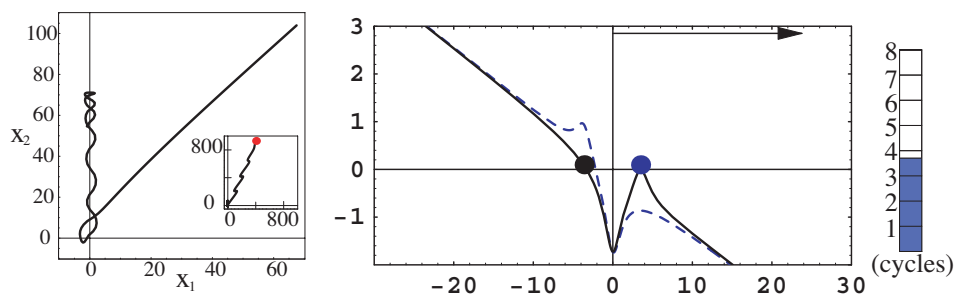


Fig. 2. Evolution of a trajectory whose final position is near the outer edge of an NSDI jet. The left panel shows the trajectory in position space, both the details near the coordinate origin during the interval 3.1 - 4.0 cycles and, in the small inset, over a wider range of positions. The red dot marks the final point at 8 cycles. Note that the scales of these two plots are different. (1.9 MB) The right panel is a single frame from the animation that shows the time development of energy and position from 3.1 to 4.0 cycles, leading to NSDI.

event. Variations on this scenario have also been suggested in which it can make a difference whether the “second” electron is initially left behind in an excited state or not, as the first electron tunnels out.

Here we suggest a reformulation of the rescattering scenario that can explain the presence of two categories of NSDI, giving zero or substantially non-zero total ion momentum peaks in a momentum distribution. Both categories have been exhibited in recent experiments. Our animations show that the returning electron, if it is accelerated by the laser force, may easily have too much energy to engage the inner electron effectively and that in this case the resulting NSDI event leads to small or zero total ion momentum (a *Z* category event). On the other hand, if the phases are such that the returning electron is retarded rather than accelerated by the laser force, its interaction with the inner electron can be surprisingly effective, leading to significant energy exchange and non-zero ion total momentum (an *NZ* category event).

In the remaining part of this paper, we illustrate the time development of zero and non-zero momentum trajectories in two separate animations. The movies included here have several points in common. The most prominent common point is that the ionization scenarios shown all have a rescattering feature. This means that one of the electrons has first been partially ejected, leaving the other near the nucleus. The “outer” electron then revisits the inner electron and prompts it to become ionized.

In the beginning of both movies, the rescattering electron, which is the “outer” one, is indicated by a blue dot or ball, while the one that is near the nucleus is indicated by a black ball. Similarly, there is a black solid curve and a blue dashed curve showing the potential energies of the bound and revisiting electrons respectively. The vertical axis labels the total energy in atomic units, and the horizontal axis plots the position in a.u. Near the top of the plot, an arrow is used to indicate the direction and magnitude of the laser force, and a thermometer located on the right of the plot shows the time during the evolution.

The left panel of Fig. 2 shows the trace of a two-electron trajectory in position space, both the details near the coordinate origin during the interval 3.1 - 4.0 cycles and, in the inset, over a wider range of positions, where the red dot marks the final point at 8 cycles. As the inset shows, both electrons emerge into the first quadrant and drift away from the nucleus in a periodic and sawtooth-type of motion. The right panel is a single frame from a movie showing the motion of both electrons during the ionizing half cycle. The result is an NSDI event in the *NZ* category.

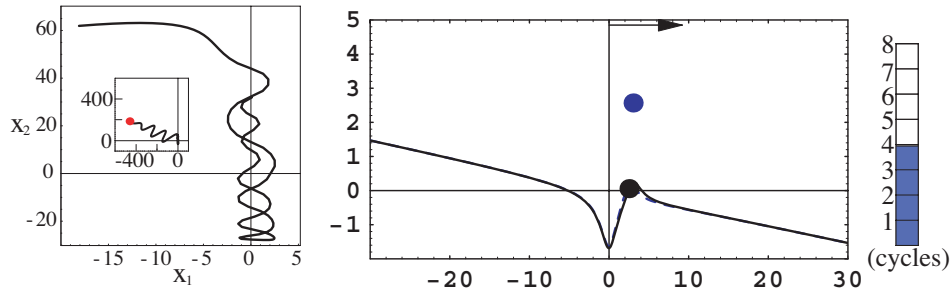


Fig. 3. Evolution of a non-jet NSDI trajectory. The large and small plots in the left panel show the time development of the two electrons in position space, during the animation time (3.4 - 4.3 cycles) and over the entire laser pulse respectively. The red dot indicates the final position of the two electrons at 8c. Note that the scale of these two plots are different. (1.9 MB) The right panel is a frame from the animation that shows the outer electron revisiting the core with high kinetic energy. The animation illustrates the time development of energy and position of two electrons from 3.4 to 4.3 cycles, leading to category Z NSDI.

By comparing the energy-position evolution of many trajectories of the same type as shown in the first movie, we find similar behavior of the rescattering electrons, even if the initial energy of the inner electron is different, for example higher than in the movie. Different inner electron bound energies lead to different values of final kinetic energy. This implies that the inner electron of an NSDI pair can be left in a variety of energies when the rescattering electron is first sent out from the nucleus. This contrasts with assumptions made in models in which the initial conditions of the outer electron are obtained through the ADK model and the initial conditions of the inner electron are assumed always to be the same, e.g. to be the ground state of He^+ as in the semiclassical calculations of L. Fu *et al.* [20].

The large and small plots in the left panel of Fig. 3 show the detailed trace of both electrons of the non-jet trajectory from 3.4 to 4.3 cycles and over the full 8-cycle pulse. A snapshot of the animation, as illustrated in the right panel of Fig. 3, shows the outer electrons leaving the nucleus with high kinetic energy.

In summary, our classical simulation shows several things. First, rescattering accompanies double ionization naturally in our approach and does not need to be initiated by tunneling. There are two relatively well distinguished scenarios that lead to two distinct categories of total electron momenta. If there is phasing that permits the laser force to slow down the rescattering electron so that it can exchange energy efficiently with the interior electron, one finds NSDI events in the category with substantially non-zero (NZ) total momenta. By contrast, trajectories in the second category of zero (Z) total momenta are of the type shown in the second movie. The important difference is the failure to achieve efficient energy exchange during recollision in the second category.

Acknowledgments

We appreciate comments by W. Becker, M.V. Fedorov, A.M. Popov, H. Rottke and W. Sandner, as well as extensive earlier interactions with S.L. Haan and R. Panfili. This research has been supported by the National Science Foundation through grant PHY00-72359 by CRDF grant RP1-2259 and by NERSC computational resources through project m197.